Workshop on Material Appearance Modeling (2016)
H. Rushmeier and R. Klein (Editors)

Interactive Appearance Prediction for Cloudy Beverages

Alessandro Dal Corso[1], Jeppe Revall Frisvad[1], Thomas Kim Kjeldsen[2], and J. Andreas Bærentzen[1]

[1]Technical University of Denmark
[2]Alexandra Institute, Denmark

Abstract

Juice appearance is important to consumers, so digital juice with a slider that varies a production parameter or changes juice content is useful. It is however challenging to render juice with scattering particles quickly and accurately. As a case study, we create an appearance model that provides the optical properties needed for rendering of unfiltered apple juice. This is a scattering medium that requires volume path tracing as the scattering is too much for single scattering techniques and too little for subsurface scattering techniques. We investigate techniques to provide a progressive interactive appearance prediction tool for this type of medium. Our renderings are validated by qualitative and quantitative comparison with photographs. Visual comparisons using our interactive tool enable us to estimate the apple particle concentration of a photographed apple juice.

Categories and Subject Descriptors (according to ACM CCS): I.3.7 [Computer Graphics]: Three-Dimensional Graphics and Realism—

1. Introduction

Quoting a food science article: "the visual appearance of a cloudy drink is a decisive factor for consumer acceptance" [Bev02]. We therefore believe that appearance prediction is highly relevant in the beverage industry of the future. It is important to predict the visual effect of a production parameter being modified, so that production parameters may be optimized without negative impact on the visual quality of the product. An appearance model also potentially enables analysis of product properties using camera sensors.

rendering photograph

Figure 1: *Cloudy apple juice photographed and rendered using our appearance model. In the model, apple particle concentration (1.0 g/L) and days the apples were stored (4) were selected to match the photograph.*

The cloudy part of a beverage typically consists of oil droplets or fruit flesh. We use Lorenz-Mie theory to go from a particle size distribution of fruit flesh particles, for example, to the scattering properties that we would use in a volume rendering [FCJ07]. Once the scattering properties are available, there are many ways to render the medium. However, in the case of a cloudy beverage, the scattering is neither low enough for single scattering techniques nor high enough for subsurface scattering techniques. We thus use full volume path tracing [Rus88], which quite accurately predicts the appearance of milk [FCJ12].

The complex refractive indices ($n = n' + i n''$) of host liquid and particle inclusions are required as input for the Lorenz-Mie theory. In many cases, these parameters depend to some degree on production parameters. In addition, the concentration of particles is often a production parameter. This enables us to build appearance models that are parameterized by production parameters. As a case study, we build such an appearance model for apple juice.

The ability to quickly test the visual influence of different parameters is one of the key advantages of material appearance prediction. This advantage is however hampered by the very long rendering times that we typically experience with full path tracing of multiple scattering in a volume. To have fast visual feedback and shorter rendering times, we use progressive path tracing implemented on the GPU using the OptiX framework [PBD*10]. We shortly cover the steps that we took to obtain an interactive appearance prediction tool based on this framework.

We validate our appearance model by qualitative comparison of rendered results with a photograph of a commercial unfiltered apple juice (Figure 1). As the visual similarity of rendered and photographed juice is better with some parameter settings than others, we can use our appearance model to roughly estimate what the parameters might have been during production of the photographed juice.

2. Appearance Model

The model we present for apple juice is intended for unfiltered press juices. Consequently, we model it simply as apple particles in clear apple juice. To obtain complex refractive indices for these constituents, we exploit that the imaginary part is directly related to the absorption of the material [FCJ07]. As we shall see in the following, the absorption of the apple particles and juice both depend on how the apples are handled, and on whether anything is done to prevent the enzymatic browning that naturally takes place when apples are peeled, bruised, or pressed in an oxidative environment.

Host. Fruit juices have a significant amount of dissolved solids (mostly sugars [HRC09]). The total concentration of soluble solids X influences the real part of the refractive index of the host. This concentration is typically measured in degrees Brix (°Bx), which is the weight percentage of dissolved solids, and it depends on the ripeness of the harvested fruits. More ripe fruits have a higher sugar content. We use two measurements from Genovese and Lozano [GL06] to find a correction for the real part of the refractive index of water. After correction, the real part of the host refractive index is

$$n'_{\text{host}}(\lambda) = n'_{\text{water}}(\lambda) + 0.0016X \ ,$$

where λ is the wavelength of the light (*in vacuo*). For the imaginary part of the refractive index, we use the different absorbance spectra of browned clarified apple juice reported by Beveridge et al. [BFH86, Fig. 4A, curve 3]. As the wavelength increases, the absorbance values become smaller and more uncertain. Since they should not decrease below the absorption of water, we convert them to absorption coefficients and gradually blend them with the absorption spectrum of water in the range of wavelengths from 400 nm to 700 nm. The spectra we get for n''_{host} as a result are in Table 1.

λ [nm]	n''_{host} 4 days	n''_{host} 9.5 days peeled	n''_{host} 9.5 days	n''_{host} 27 days	n''_{part}
375	$1.58 \cdot 10^{-6}$	$1.03 \cdot 10^{-6}$	$2.20 \cdot 10^{-6}$	$3.20 \cdot 10^{-6}$	$1.14 \cdot 10^{-5}$
400	$1.69 \cdot 10^{-6}$	$1.10 \cdot 10^{-6}$	$2.35 \cdot 10^{-6}$	$3.41 \cdot 10^{-6}$	$1.02 \cdot 10^{-5}$
425	$6.78 \cdot 10^{-7}$	$8.92 \cdot 10^{-7}$	$1.39 \cdot 10^{-6}$	$2.78 \cdot 10^{-6}$	$1.08 \cdot 10^{-5}$
450	$4.47 \cdot 10^{-7}$	$8.25 \cdot 10^{-7}$	$1.17 \cdot 10^{-6}$	$2.68 \cdot 10^{-6}$	$1.15 \cdot 10^{-5}$
475	$4.08 \cdot 10^{-7}$	$7.18 \cdot 10^{-7}$	$9.79 \cdot 10^{-7}$	$2.19 \cdot 10^{-6}$	$9.83 \cdot 10^{-6}$
500	$3.97 \cdot 10^{-7}$	$5.50 \cdot 10^{-7}$	$7.33 \cdot 10^{-7}$	$1.44 \cdot 10^{-6}$	$8.36 \cdot 10^{-6}$
525	$3.51 \cdot 10^{-7}$	$3.65 \cdot 10^{-7}$	$5.06 \cdot 10^{-7}$	$8.71 \cdot 10^{-7}$	$3.59 \cdot 10^{-6}$
550	$2.53 \cdot 10^{-7}$	$2.43 \cdot 10^{-7}$	$3.04 \cdot 10^{-7}$	$5.05 \cdot 10^{-7}$	$2.54 \cdot 10^{-6}$
575	$1.67 \cdot 10^{-7}$	$1.67 \cdot 10^{-7}$	$1.84 \cdot 10^{-7}$	$3.09 \cdot 10^{-7}$	$1.92 \cdot 10^{-6}$
600	$1.06 \cdot 10^{-7}$	$1.13 \cdot 10^{-7}$	$1.13 \cdot 10^{-7}$	$1.90 \cdot 10^{-7}$	$1.52 \cdot 10^{-6}$
625	$6.78 \cdot 10^{-8}$	$8.22 \cdot 10^{-8}$	$7.64 \cdot 10^{-8}$	$1.18 \cdot 10^{-7}$	$1.41 \cdot 10^{-6}$
650	$4.74 \cdot 10^{-8}$	$6.23 \cdot 10^{-8}$	$5.24 \cdot 10^{-8}$	$7.22 \cdot 10^{-8}$	$1.47 \cdot 10^{-6}$
675	$3.70 \cdot 10^{-8}$	$4.63 \cdot 10^{-8}$	$3.91 \cdot 10^{-8}$	$4.58 \cdot 10^{-8}$	$1.78 \cdot 10^{-6}$
700	$3.48 \cdot 10^{-8}$	$3.48 \cdot 10^{-8}$	$3.48 \cdot 10^{-8}$	$3.48 \cdot 10^{-8}$	$6.13 \cdot 10^{-7}$
725	$8.59 \cdot 10^{-8}$	$8.59 \cdot 10^{-8}$	$8.59 \cdot 10^{-8}$	$8.59 \cdot 10^{-8}$	$2.08 \cdot 10^{-7}$
750	$1.47 \cdot 10^{-7}$	$1.47 \cdot 10^{-7}$	$1.47 \cdot 10^{-7}$	$1.47 \cdot 10^{-7}$	$1.78 \cdot 10^{-7}$
775	$1.49 \cdot 10^{-7}$	$1.49 \cdot 10^{-7}$	$1.49 \cdot 10^{-7}$	$1.49 \cdot 10^{-7}$	$1.58 \cdot 10^{-7}$

Table 1: *Absorption of clarified apple juice (host) and apple flesh (particles) reported in the form of the imaginary part of the index of refraction.*

Particles. We model the apple particles as browned apple flesh. The real part of the refractive index of the apple particles was estimated by Benitez et al. [BGL07] to be $n'_{\text{part}}(\lambda) = 1.487$. For the imaginary part, we use the absorption spectrum measured by Lu et al. [LCHA10] for bruised apple tissue (two days after bruising). These measurements are in the range of wavelengths from 500 nm and up. For the shorter wavelengths, we use the absorption spectrum measured for apple flesh by Saeys et al. [SVRT*08]. The two curves fit fairly well together, so we assume that the bruising mostly affects absorption at wavelengths from 500 nm and up. The combined spectrum that we use is in Table 1. The size distribution of the apple particles is typically bimodal [Bev02]. Smaller particles (diameter of less than around 0.65 μm) will stay suspended, while larger particles will sediment during storage and will require the juice to be shaken to be resuspended. We use a bimodal particle size distribution measured for a centrifuged apple juice [ZPDG94, Bev02].

3. Rendering Method

Our outset is unidirectional path tracing [Kaj86, PH10]. We use Russian roulette to terminate paths probabilistically (based on material absorption) and to choose between reflection and refraction in the case of transparent materials [AK90]. Our scene is composed of four different kinds of materials: emissive, diffuse, glass, and liquid. For accurate rendering, we assign liquid/air, glass/air, and liquid/glass interfaces to the specular surfaces in our scene.

Assuming that the specular surfaces are perfectly smooth, we use the laws of reflection and refraction for their path tracing with Fresnel reflectance as the probability of reflection [PH10]. We also account for glass absorption using an RGB absorption coefficient for crown glass $\sigma_{a,\text{glass}} = (0.234, 0.233, 0.376)$ that we calculated from the imaginary part of the refractive index of Schott N-K5 glass. The

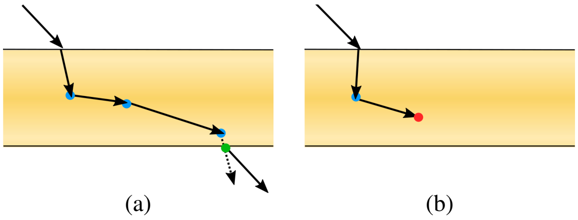

Figure 2: *The scattering process using shadow rays. Each shadow ray has a sampled direction (sampled with the Henyey-Greenstein phase function) and length (from an exponential distribution of average σ_t). In (a), the random walk exits the material and continues path tracing. In (b), the last ray is absorbed and the random path discarded.*

average over the color bands of the beam transmittance $T_r = e^{-\sigma_{a,\text{glass}} s}$, where s is the distance traveled through the glass medium, is then the probability that the path continues through the glass without being terminated.

The cloudy beverage is also considered a specular material, but it also contains light scattering particles. When a ray passes through this medium (either by refracting into it or by internal reflection), we perform a volumetric scattering process as illustrated in Figure 2. This is done by a stochastic walk inside the medium based on the scattering properties (scattering and extinction coefficients, σ_s and σ_t, and asymmetry parameter, g) that we obtain from the Lorenz-Mie theory. At each step of the walk, we use the scattering albedo σ_s/σ_t in a Russian roulette as the probability of the path surviving without being absorbed. We discard the whole walk if the ray is absorbed. If the ray is not absorbed, we sample the distance to the next scattering event using $s = \ln(-\xi)/\sigma_t$, where $\xi \in [0,1)$ is a uniform random variable. If s is beyond the surface of the medium, the next scattering event is interaction with the surface in the usual way. If not, we sample a new scattering direction using the Henyey-Greenstein phase function [PH10] (which is a function of g). To improve efficiency, we randomly pick one RGB components when performing the scattering process, and all tracings inside the medium are done with shadow rays using the distance to the next scattering event as the maximum trace distance.

4. Materials

To capture a reference photograph, we set up a scene consisting of a drinking glass with unfiltered apple juice placed on a neutral white surface with a neutral white background. The glass was illuminated by a large diffuse light source at a 45° angle. We used a standard digital single-lens reflex (DSLR) camera with a 50 mm lens. The light source was a Bowens BW3370 100W Unilite, which is a compact fluorescent light source with a correlated color temperature (CCT) of 6400 K. This is fairly close to the equal energy point (E with $x = y = 1/3$) in the chromaticity diagram, which is also the reference white point of the CIE RGB color space. We thus model our light source as being purely white, and convert the spectral optical properties obtained from our appearance model to CIE RGB using the RGB color matching functions reported by Stockman and Sharpe [SS00].

	4 days	9.5 days peeled	9.5 days	27 days
0.0 g/L	0.1333	0.1337	0.1508	0.2015
0.1 g/L	0.0480	0.0649	0.1025	0.1741
0.2 g/L	0.0411	0.0657	0.1048	0.1753
0.5 g/L	0.0368	0.0689	0.1072	0.1755
1.0 g/L	**0.0363**	0.0687	0.1055	0.1731
2.0 g/L	0.0416	0.0563	0.0858	0.1519

Table 2: *RMSE for a patch of color in the lower part of the glass. We note a minimum error around the 0.5-1.0 g/L concentration and 4 days storage time.*

The apple juice is an unfiltered press juice from Orskov Foods with a sugar content of 10 g per 100 ml. We estimated $X = 11.25$ as the juice also contains pectin, organic acids, and salts in addition to the sugar [GL06], and with this X we get n'_{host} equal to one previously measured for regular pressed cloudy apple juice [BGL07].

5. Results

We performed two sets of comparisons, one qualitative in Figures 1 and 3 and one quantitative in Table 2. All comparisons show the converged result after 5000 accumulated frames. On a qualitative visual comparison, the photograph matches most closely the rendering with concentration in the 0.5-1.0 g/L range and a storage time of 4 days. For the quantitative comparison, we compare a patch of color on the lower part of the glass. As a metric, we use the RMSE of the color bands on the patch. The quantitative result places the concentration between 0.5 g/L and 1.0 g/L, slightly leaning towards the latter and confirming our qualitative comparison. Strong highlights in the glass are due to rays getting trapped due to total internal reflection.

Our implementation of the method, based on OptiX [PBD*10], runs progressively on the GPU, with an average frame rate of 12 frames per second on an NVIDIA GeForce 780 Ti card. This enables us to get nearly converged results in less than 10 minutes. A visual comparison of the main liquid is possible within a minute (~600 frames), while caustics from the juice take much longer to converge.

6. Discussion

By combining existing techniques in our framework, we enable interactive testing of the influence of different production parameters on the appearance of a cloudy beverage. Our case study enables approximate simulation of the appearance

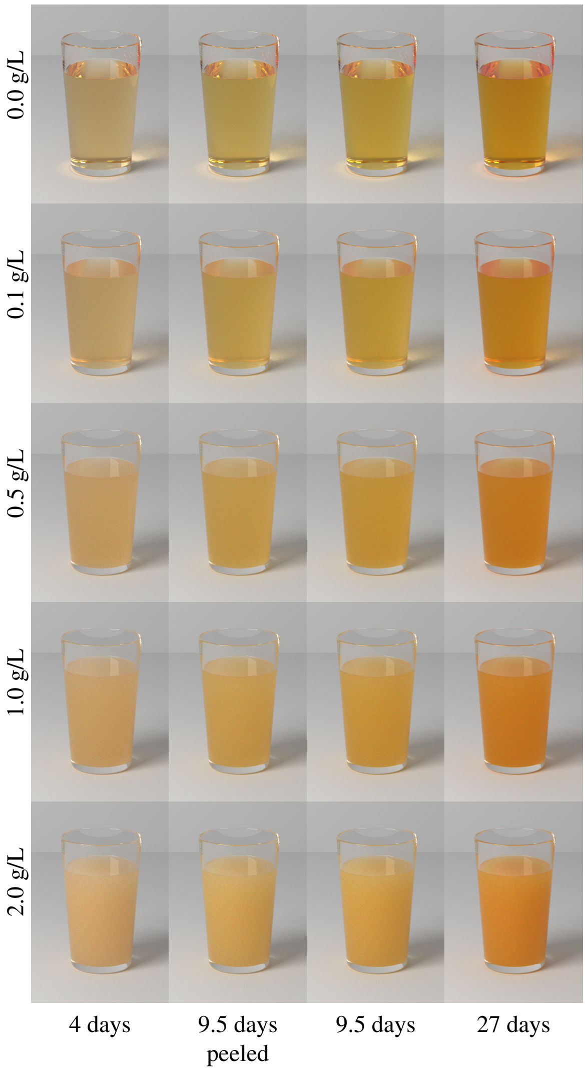

Figure 3: *Visual comparison of our renderings varying two parameters: particle concentration and apple storage time.*

of cloudy apple juice during production. However, we cannot match the photograph perfectly, and can thus only give a rough estimate of the parameters. As a possible future step, we want to improve precision by better estimating scene geometry, camera parameters, and lighting environment.

Acknowledgements. Thanks to Anders Wang Kristensen for setting up a digital scene to match the photographed scene, and to him and Marek Krzysztof Misztal for their help with respect to capture of the reference images.

References

[AK90] ARVO J., KIRK D.: Particle transport and image synthesis. *Computer Graphics (Proceedings of SIGGRAPH '90) 24*, 4 (August 1990), 63–66. 2

[Bev02] BEVERIDGE T.: Opalescent and cloudy fruit juices: Formation and particle stability. *Critical Reviews in Food Science and Nutrition 42*, 4 (2002), 317–337. 1, 2

[BFH86] BEVERIDGE T., FRANZ K., HARRISON J. E.: Clarified natural apple juice: Production and storage stability of juice and concentrate. *Journal of Food Science 51*, 2 (March 1986), 411–433. 2

[BGL07] BENITEZ E. I., GENOVESE D. B., LOZANO J. E.: Scattering efficiency of a cloudy apple juice: Effect of particles characteristics and serum composition. *Food Research International 40*, 7 (August 2007), 915–922. 2, 3

[FCJ07] FRISVAD J. R., CHRISTENSEN N. J., JENSEN H. W.: Computing the scattering properties of participating media using Lorenz-Mie theory. *ACM Transactions on Graphics (Proceedings of SIGGRAPH 2007) 26*, 3 (July 2007), 60:1–60:10. 1, 2

[FCJ12] FRISVAD J. R., CHRISTENSEN N. J., JENSEN H. W.: Predicting the appearance of materials using Lorenz-Mie theory. In *The Mie Theory: Basics and Applications*, Hergert W., Wriedt T., (Eds.), vol. 169 of *Springer Series in Optical Sciences*. July 2012, ch. 4, pp. 101–133. 1

[GL06] GENOVESE D. B., LOZANO J. E.: Contribution of colloidal forces to the viscosity and stability of cloudy apple juice. *Food Hydrocolloids 20*, 6 (August 2006), 767–773. 2, 3

[HRC09] HUANG Y., RASCO B. A., CAVINATO A. G.: Fruit juices. In *Infrared Spectroscopy for Food Quality Analysis and Control*, Sun D.-W., (Ed.). Academic Press/Elsevier, 2009, ch. 13, pp. 355–375. 2

[Kaj86] KAJIYA J. T.: The rendering equation. *Computer Graphics (Proceedings of SIGGRAPH 86) 20*, 4 (August 1986), 143–150. 2

[LCHA10] LU R., CEN H., HUANG M., ARIANA D. P.: Spectral absorption and scattering properties of normal and bruised apple tissue. *Transactions of the American Society of Agricultural and Biological Engineers 51*, 1 (2010), 263–269. 2

[PBD*10] PARKER S. G., BIGLER J., DIETRICH A., FRIEDRICH H., HOBEROCK J., LUEBKE D., MCALLISTER D., MCGUIRE M., MORLEY K., ROBISON A., STICH M.: OptiX: a general purpose ray tracing engine. *ACM Transactions on Graphics (Proceedings of SIGGRAPH 2010) 29*, 4 (July 2010), 66:1–66:13. 2, 3

[PH10] PHARR M., HUMPHREYS G.: *Physically Based Rendering: From Theory to Implementation*, second ed. Morgan Kaufmann/Elsevier, 2010. 2, 3

[Rus88] RUSHMEIER H. E.: *Realistic image synthesis for scenes with radiatively participating media*. PhD thesis, Cornell University, Ithaca, NY, USA, 1988. 1

[SS00] STOCKMAN A., SHARPE L. T.: The spectral sensitivities of the middle- and long-wavelength-sensitive cones derived from measurements in observers of known genotype. *Vision Research 40*, 13 (2000), 1711–1737. 3

[SVRT*08] SAEYS W., VELAZCO-ROA M. A., THENNADIL S. N., RAMON H., NICOLAI B. M.: Optical properties of apple skin and flesh in the wavelength range from 350 to 2200 nm. *Applied Optics 47*, 7 (March 2008), 908–919. 2

[ZPDG94] ZIMMER E., PECORONI S., DIETRICH H., GIERSCHNER K.: Process technological and chemical basis of the production of cloudy apple juice, also considering continuous processes. I. Contributions to the chemical analysis of natural cloudy apple juices including physical parameters. Part II. *Die industrielle Obst- und Gemüseverwertung 79*, 12 (1994), 426–434. 2